

STABILITY MEASUREMENTS OF A LARGE Nb₃Sn

FORCE-COOLED CONDUCTOR*

J. R. Miller, J. W. Lue, S. S. Shen, and L. Dresner
Oak Ridge National Laboratory, Oak Ridge, Tennessee 37830

MASTER

Introduction

The Westinghouse coil for the Large Coil Program (LCP) at ORNL will use a cable-in-conduit conductor made of copper-stabilized, multi-filamentary (MF) Nb₃Sn strands enclosed in a stainless steel jacket. The operating current will be 16 kA with an 8-T maximum field. The stainless steel jacket provides a channel around the conductor to allow forced cooling by supercritical helium. In this study we investigate the performance of a subsize conductor similar in construction, but with only one-third as many active strands in the cable.

Test Conductor Description

A detailed characterization of the test conductor is given in Table I. The subsize cable in this conductor was formed by three successive triplexing steps to form subcables, followed by cabling of six subcables with active strands around a seventh subcable having all copper strands. The cable was compacted after jacketing to leave ~35% of the cable space void and available for interstitial flow of helium.

Table I. Conductor Description

Conductor type	Cable-in-conduit
----------------	------------------

*Research sponsored by the Office of Fusion Energy, U.S. Department of Energy, under contract W-7405-eng-26 with the Union Carbide Corporation.

Table I. Conductor Description (Cont'd)

Cable pattern	6 \times 5 ³ MF Nb ₃ Sn composite strands around a core of 5 ³ all copper strands
Strand diameter	0.69 mm
Copper/noncopper ratio in the composite strands	1.9/1
Jacket material	304L stainless steel
Jacket dimensions	(12.5 mm) ² outside with 2.8-mm outside corner radii and 0.79-mm wall
Available cable space	1.17 cm ²
Effective conductor cross section	0.76 cm ²
Cable void fraction	35%
Test conductor heated length	4 85-cm sections; 3.4 m total
Single strand critical current	122 A at 8 T, 4.2K*
Full conductor quench current	19.7 kA at 8 T, 4.2K

*This current represents an effective resistivity of $2 \times 10^{-12} \Omega \text{ cm}$ in a control sample reacted simultaneously with the test conductor.²

The strands in this test conductor were bare except for a thin oxide layer apparently caused by inadvertent exposure of the conductor to air at some point in the heat treatment used to form Nb₃Sn. Though unintentional, this oxidization seems to have minimized sintering between strands.

Experimental Approach

There were two important goals in testing the subsize conductor:

(1) to determine whether the current capacity of a finished conductor of this type could be related to the critical current of a single strand,

and (2) to measure the stability margin of the conductor, i.e., the sudden input of energy from which such a conductor will just recover under given conditions of current, field, and helium flow.

Test configuration

Because of the physical size and current capacity of the conductor and fragile nature of the Nb_3Sn filaments, arranging and supporting the test sample in a high background field required care. We bent the sample, prior to reaction, into a large "paper clip" shape with four straight sections roughly 0.6 m long separated by 0.15-m-radius bends. A background field up to 8 T was provided by a split solenoid pair, which had iron cores for enhancement of the central field and improvement of field uniformity over the 150-mm-diam. high field region. The halves of the solenoid pair are separable and the gap adjustable allowing the sample to be positioned in it with two straight legs of the paper clip passing through the high field region.

Current leads were connected to the encapsulated cable by copper tubes swaged down over the cable ends before reaction, a process developed for such conductors by Airco. Over these swaged ends were soldered large copper lugs with fitted tubes and internal plenums which allow helium to be injected into the cable. Before the current lugs were installed, 96 axial field pulse coil segments were slipped over the conductor so that most of its length could be heated.

Shown in Fig. 1 is the bent and reacted test conductor with one lug and all the pulse coil segments in place and lying in a steel channel that is part of the separator structure of the solenoid pair. At the end where the lug was still not installed, a section of cable is visible between the swaged end and the sheath into which helium must enter from

the plenum. Figure 2 shows the test conductor positioned on one-half of the solenoid pair. A shroud was constructed around those parts of the conductor not inside the magnet structure for constraint against the high magnetic forces. Small voids between the conductor exterior, the pulse coils, the shroud, and the magnet structure were filled with a low melting wax to spread loads, to provide thermal isolation between conductor interior and helium bath, and to improve electrical insulation between pulse coil leads and other apparatus. When fully assembled, the split solenoid test conductor unit was hung with the paper clip sample in a vertical plane, the current lugs being uppermost.

A 20-V, 30-kA SCR power supply provided dc current. Vapor-cooled leads rated at 20 kA carried current to the conductor. Helium flow was supplied by a blowdown system similar to that previously described^{3,4} but scaled up in capacity.

Heating method for stability testing

Tests of conductor stability require that a known amount of energy be deposited into a volume of conductor while it is operating under otherwise fixed conditions. We monitored conductor voltage to observe momentary transitions to the normal state and to determine whether the conductor was able to recover the superconducting state after the energy deposition. The highest energy deposition per unit volume of conductor from which recovery was just possible is called the stability margin for the given conditions. The task of injecting heat into an encapsulated cable is difficult, and the difficulty is compounded by the necessity of performing the reaction heat treatment after constructing and forming the test sample. For this test we chose an induction heating method

using pulse coils around the conductor exterior. Energy was supplied to the pulse coils by a capacitive discharge using SCR switching.

The pulse coils themselves were wound in short segments with lengths and inside dimensions selected to allow them to slip around the bends of the preformed sample. Ninety-six segments were used, but these were divided into four separate banks, each bank powered by an independent section of the capacitive discharge supply. Each bank contained parallel combinations of eight sets of three series-connected coil segments. Details of pulse coil and power supply design and operation will be given elsewhere,⁵ but for the purpose of this paper the schematic representation of Fig. 3 suffices.

The schematic represents one bank of pulse coils surrounding an 85-cm section of conductor. Recall from Table 1 that the effective conductor cross section is 0.76 cm^2 so that about 65 cm^3 of conductor is contained in one bank of pulse coils. As shown, the pulse field is applied parallel to the direction of the transport current.

The inset of Fig. 3 contains the record of a typical discharge. In this case the initial capacitor voltage was 900 V resulting in a maximum field of 0.8 T and maximum field swing of 1.4 T in 0.9 ms. From the initial and final capacitor voltages we know the total energy discharged.

To determine the partition of pulse energy among the test conductor, the pulse coil and its leads, and the surrounding structure, separate measurements were done using ac loss techniques. Of the energy of any discharge, about 73% is deposited in the conductor, 10% goes to the pulse coils and external leads, and the remainder is lost to the surrounding structure.⁵

The energy deposited in the stainless steel jacket is negligible in the

present case so that 1.43 J/cm^3 of conductor is the energy deposition in this example. From Fig. 3 we see that most of the energy is deposited within a few milliseconds.

Results and Discussion

The data for stability margin vs transport current at 8-T applied field are plotted in Fig. 4. The internal helium was pressurized to 5 atm but had no imposed flow. The temperature was that of the external bath, 4.2K. The open circles represent recovery, all pulse coils being simultaneously energized. The solid circles correspond to pulsing only those coils on a straight section near the center of the sample and passing through the high field region. Comparison of the two sets of data demonstrates an effect of heated length. Over the current range investigated, the energy required to produce an irreversible quench was $400-500 \text{ mJ/cm}^3$ higher when only one-fourth rather than the total sample was heated. A word of caution is in order. When the total sample was heated, both sections in high field were affected. We do not know how the separation of the two high field regions influences the total conductor stability.

The solid curve in Fig. 4 represents the available enthalpy of the internal helium between its initial temperature and the current sharing temperature of the conductor if only constant pressure processes are considered. It is apparent that more energy has been absorbed in bringing about recovery in the events represented by the data. We have observed similar phenomena repeatedly in the past and attribute the difference to effects of pressure and flow transients produced by the heat pulse. In the present experiment, the difference may have been accentuated by the

short (15-cm) length exposed to high field. Qualitatively though, the data do exhibit the same current dependence as the available enthalpy. The high stability margin leads to the inference that heat transfer from the cable to the bulk of the internal helium was good enough, even with no imposed flow, to make practically all the helium in the heated region available for recovery. Cursory checks on the flow and pressure dependence of the stability margin did not produce observable differences in the data. It has already been pointed out⁶ that because of the higher critical temperature of Nb_3Sn , there should be no advantage to operating at pressures lower than 5 atm.

The limits of stability were not obtainable at currents below 12 kA because the design limits of the capacitive discharge supply and pulse coil system had already been reached. Another limit, that of the current leads, was also approached in measuring the sample current capacity. During a slow current ramp, a spontaneous quench occurred at 19.7 kA, a value that is within 1% of the extrapolated single strand critical current.

In previous experiments with NbTi conductors of similar construction, multiple stability regimes were observed.⁴ In particular, in a plot of stability margin vs current, an upper and lower limit might exist. A careful search was conducted for lower regions of instability in the present experiment and none was found. The nature of the observed quench above the measured stability limit convinced us that there were also no higher regions of stability. The theory⁴ constructed to describe the mechanisms behind our previous experimental results can be used to show that what has been observed in these experiments is the upper stability margin and that the lower limit should not exist for our experiment.

Figure 5 shows a schematic representation of the stability margin, ΔH , as a function of imposed helium flow, v , and transport current, I . The surface has a fold near the points A, B, F, and K that makes the stability margin multivalued. The existence of the fold has been inferred from the two kinds of stability curves we observed earlier.⁴ If we slice the stability surface through the fold with a plane parallel to the H-I plane, we get a Z-shaped curve, whereas if we slice through the fold with a plane parallel to the H-v plane, we get a smooth curve lying above a pair of intersecting segments. Point B on the stability surface determines the limiting current, I_{\lim} , below which the stability margin is always single-valued and equal to the upper stability margin. According to the theory of Ref. 4, the current density at point B scales as

$$J_{co} \sim [f(1 - f_{co})/f_{co}]^{1/2} (T_{cr} - T_b)^{1/2} \rho^{-1/2} t^{-1/5} \ell^{2/5} D^{-1} \quad (1)$$

where

J_{co} = the current density in the metal strands of the conductor (Am^{-2}),

f = the volume fraction of copper in the metal,

f_{co} = the volume fraction of metal in the cable space,

T_{cr} = the critical temperature (K),

T_b = the ambient helium temperature (K),

ρ = the resistivity of the copper including magneto-resistance ($\Omega \text{ m}$),

t = the duration of the normalizing heat pulse (s),

ℓ = the length of the heated zone (m),

D = the hydraulic diameter of the helium filled part of the cable space (m).

We can use relation (1) to scale the results of Ref. 4 to the conditions of the subsize conductor tests. The result is $I_{lim} = 28$ kA, which is above the critical current. In such a case, the stability margin is always single-valued and equal to the upper stability margin. The main reasons that I_{lim} for the subsize cable is much higher than for the experiments of Ref. 4 are the larger value of $T_{cr} - T_b$ for Nb_3Sn compared with NbTi and the smaller hydraulic diameter of the subsize cable.

Conclusion

The measured quench current of 19.7 kA at 8 T is within 1% of the extrapolated single strand critical current. This definitely enhances one's confidence in the manufacturability of Nb_3Sn cable-in-conduit superconductors. A high stability margin ($\gtrsim 0.7$ J/cm³ for J_{cable} space ≤ 13.6 kA/cm²) can be expected for this type conductor under operating conditions similar to the present experiment. No low lying instability regime is expected or was observed. A stability margin higher than the available constant-pressure enthalpy confirmed our previous experience.

ACKNOWLEDGMENTS

The authors gratefully acknowledge the support of technicians L. Alley and J. P. Rudd in instrumenting and operating this experiment. We also wish to thank craftsmen H. C. DeArmond, B. C. Smith, P. G. Doberstein, and R. Dixon for skillful construction of the apparatus.

REFERENCES

1. P. N. Haubenreich, J. N. Luton, and P. B. Thompson, IEEE Transactions on Magnetics, MAG-15(1): 520 (1979).
2. P. A. Sanger, Airco, Inc., private communication (1978).
3. J. R. Miller, J. W. Lue, S. S. Shen, and J. C. Lottin, IEEE Transactions on Magnetics, MAG-15(1): 351 (1979).
4. J. W. Lue, J. R. Miller, and L. Dresner, "Stability of Cable-in-Conduit Superconductors," submitted for publication to J. Appl. Phys.
5. R. B. Easter, J. R. Miller, and S. S. Shen, "Development of a Pulsed Heating Technique for Stability Testing in the Westinghouse LCP Coil," submitted to the Eighth Symposium on Engineering Problems of Fusion Research.
6. L. Dresner and J. W. Lue, Proc. of the Sixth Int'l. Conf. on Magnet Technology, Bratislava, Czechoslovakia, 1977, p. 1045.

FIGURE CAPTIONS

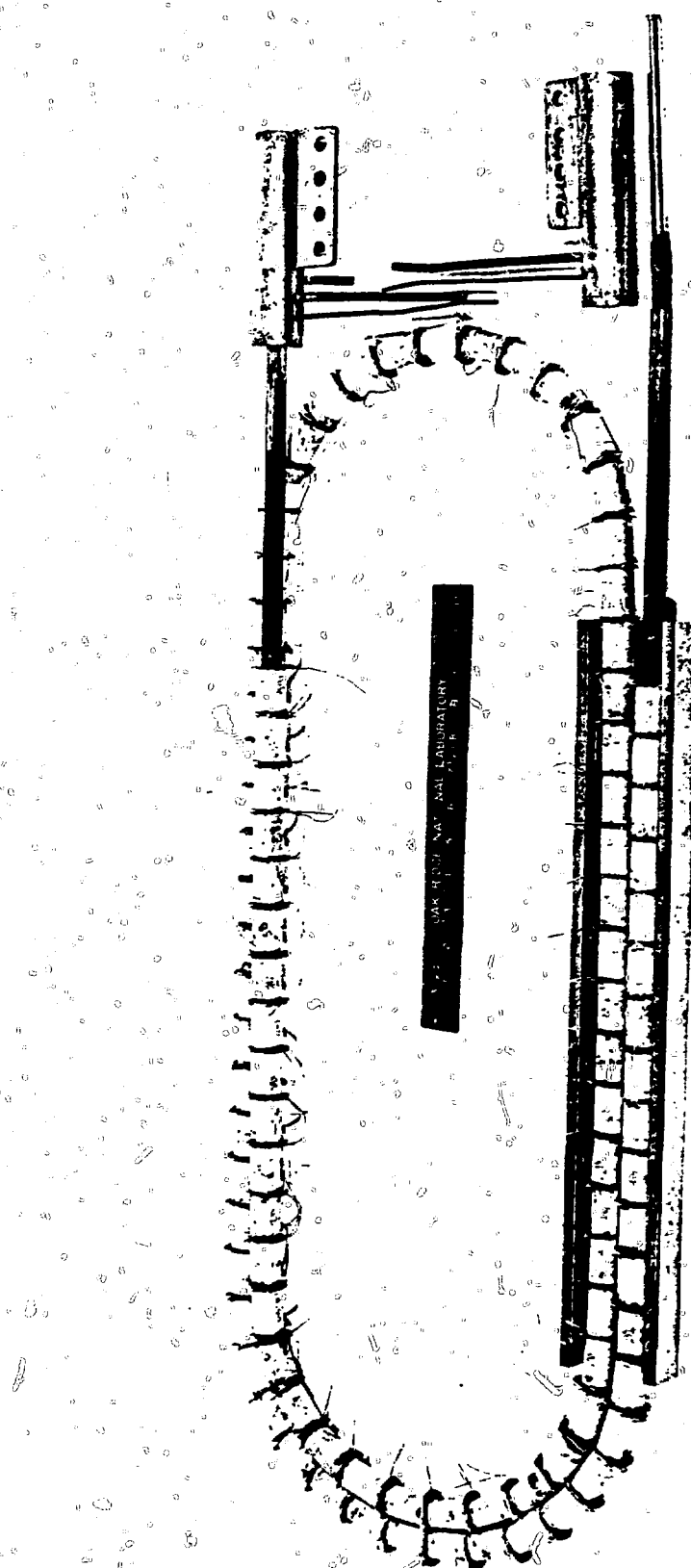
Fig. 10 Bent and reacted test conductor showing pulse coil segments and current lugs.

Fig. 2 Test conductor positioned on one half of the solenoid pair.

Fig. 3 Schematic representation of the pulse coil with typical pulse coil voltage and field traces. Time scale for the traces is 1 ms/div. Voltage scale is 200 V/div and field scale is 0.28T/div.

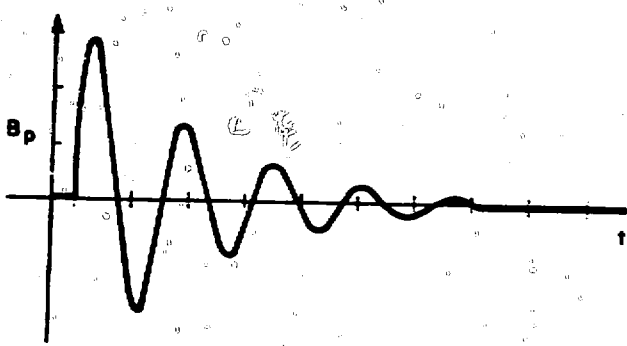
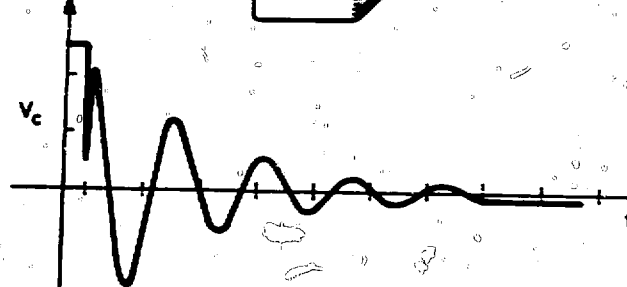
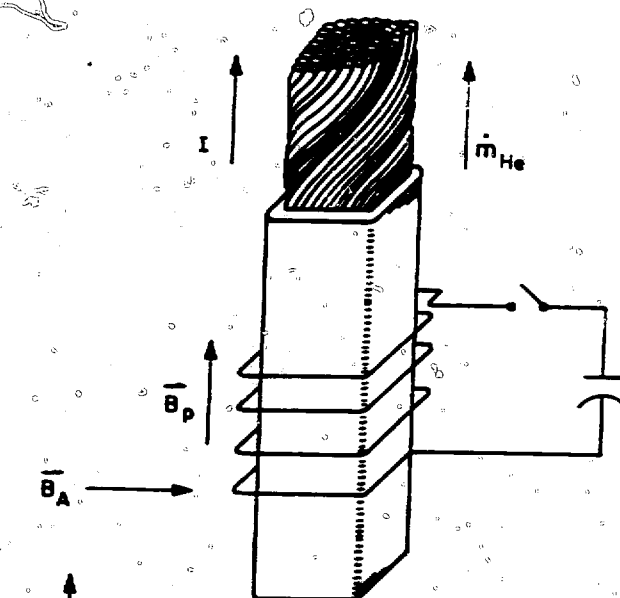
Fig. 4 Stability margin at 8 T as a function of transport current.

Fig. 5 Schematic representation of the stability margin as a function of imposed helium flow and transport current. The fold in the stability surface is connected with the occasional multivaluedness of the stability margin.

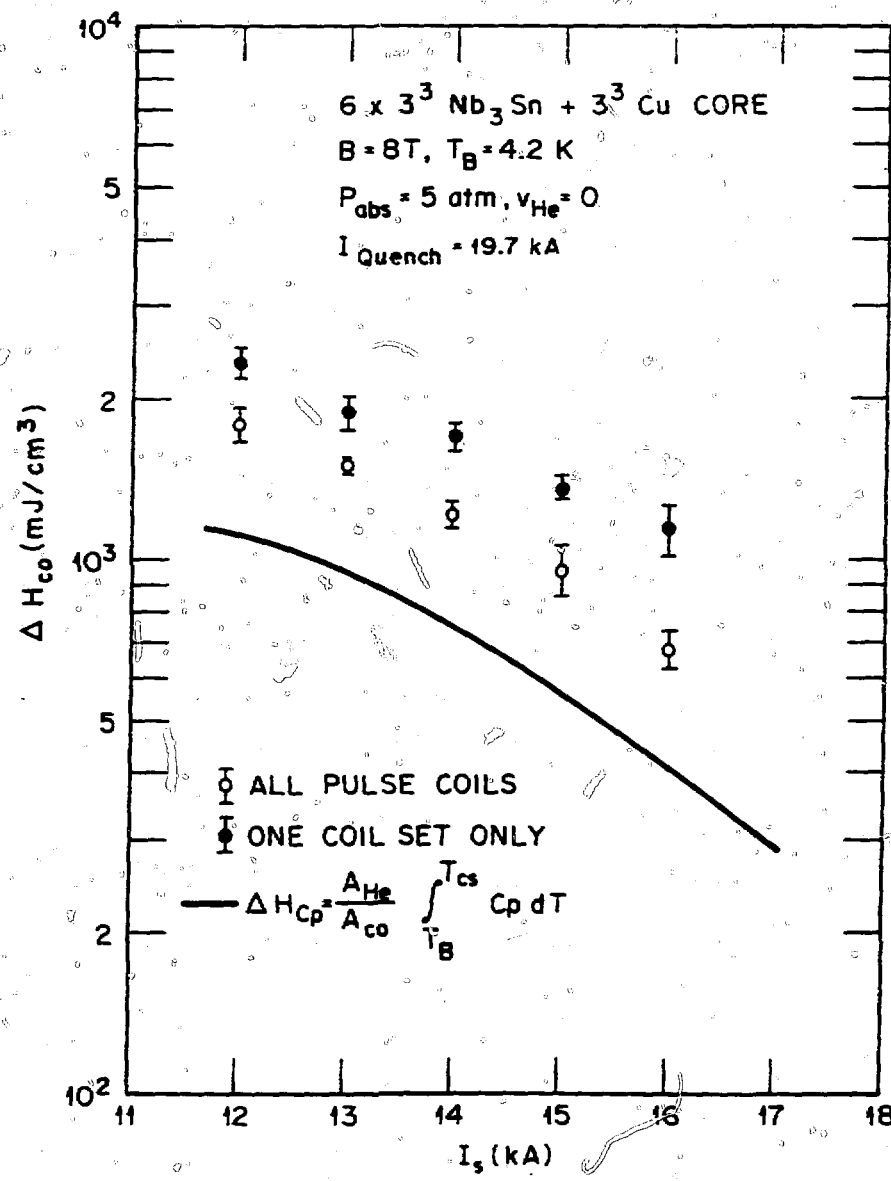




ORNL-DWG 79-2751 FED



ORNL-DWG 79-2694 FED



ORNL DWG 79-2773 FED

